Nanoscale

Accepted Manuscript

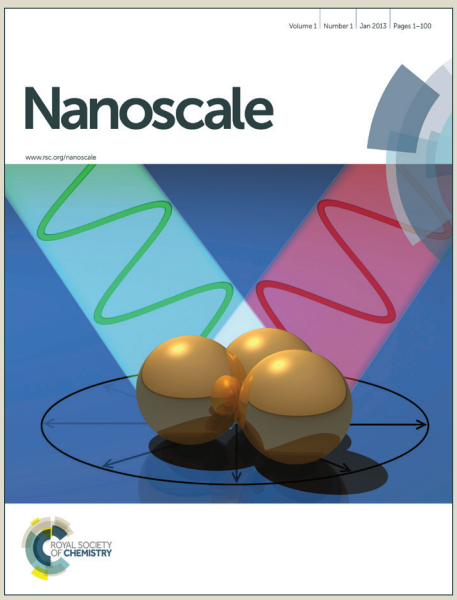

ROYAL SOCIETY OF CHEMISTRY

www.rsc.org/nanoscale

Surface plasmon coupled metal enhanced spectral and charge transport properties of Poly (3, 3‴- dialkylquarterthiophene) Langmuir Schaefer film.

Rajiv K. Pandey [a], Swatantra K. Yadav[b], Chandan Upadhyay, [a] Rajiv Prakash [a] and Hirdyesh Mishra [b *]

[a] School of Materials Science and Technology, Indian Institute of Technology (BHU), and

[b]Department of Physics, MMV, Banaras Hindu University, Varanasi-221005, India

Abstract

The coupling of organic molecules excitons with metal nano-structure surface plasmons can improve the performance of optoelectronic devices. This paper presents the effect of localized silver metal surface plasmons on spectral as well as charge transport properties of ordered molecular Langmuir Schaefer (LS) films of a fluorescent conducting multifunctional organic polymer: Poly (3, 3‴- dialkylquarterthiophene) [PQT-12]. Stability and thickness of PQT-12 LS film were studied by pressure vs. area isotherm curve. Atomic force microscopic images indicate the formations of smooth ordered polymer thin LS film of PQT-12 over silver nano structure islands films [SNIF] (~ 40 to 50 nm in size). Raman, electronic absorption and fluorescence spectral measurements of PQT-12 LS film, near SNIF i.e. the near field, shows plasmon coupled enhancement of ~13 fold in intensity of Raman bands along with two fold enhancement in absorption band (531 nm) and six fold enhancement in fluorescence band (665 nm) coupled with decrease in fluorescence decay time with improved photo-stability as compared to an identical control sample containing no SNIF i.e. the far field condition. These results indicate the formation of plasmon coupled unified fluorophor system due to adsorption of PQT-12 LS film over SNIF. The effect of plasmonic coupling is also studied by applying electric field in sandwiched structures of Al/PQT-12 LS/SNIF/ITO

with respect to Al/PQT-12 LS/ITO. Nearly three order of magnitude enhancement in current density (J-V plot) of PQT-12 LS film is observed in presence of SNIF, which further increases, on illuminating the film by green laser light [532 nm], while florescence intensity and decay time decreases. X-ray photoelectron spectroscopic measurement of SNIF also shows a red shift in $3d_{3/2}$ and $3d_{5/2}$ transitions of silver in PQT-12 coated LS film, which indicates partial charge transfer from PQT-12 polymer backbone to SNIF and causes enhancement in conductivity. This again supports the formation of field controlled radiating plasmon coupled fluorophor unified system. These findings shows greater potential in developing a voltage controlled high photon flux electroluminescence material for multifarious applications.

Key words- Siver Nano Island films, Surface enhance absorption and emission, Surface Plasmon, Plasmon-enhanced fluorescence, Charge transport, Partial charge transfer.

*Corresponding author email- hmishra@bhu.ac.in

1 Introduction

Nowadays, significant efforts have been directed to improve the efficiency of organic polymer-based electronic and optoelectronic devices using a variety of processing strategies. However, the performance of these devices is not yet up to the benchmark. Recently, near field surface plasmon interaction opened up an opportunity to improve the efficiency of these devices by adding plasmonic nano materials in ordered organic polymer films.[1-3] The incorporation of plasmonic nano materials in devices cause interactions between the surface plasmons of metal nano structures and excitons of organic molecules, which gives rise to a number of interesting phenomena and a wide range of technological applications such as surface enhanced Raman spectroscopy, plasmon-enhanced fluorescence, plasmon-enhanced solar light harvesting large panels, improved organic LED and ultrasensitive chemical and biological sensors.[4-11]

Surface plasmons are collective oscillations of free electrons in a metal nanostructure at an interface with a dielectric. Excitation of surface plasmons of nano structure by light, at which resonance occurs, can result in strong light scattering with the appearance of intense surface plasmon absorption bands and an enhancement of the local electromagnetic fields. The coupling effect between excitons and surface plasmons, which is caused by the overlap of the local electromagnetic field of excitons in polymeric layer and surface plasmons, leads to the significant radiative emission through effective energy transfer. In addition, metal nanoparticle can act as effective antennas for incident light, enabling the storage of the incident energy in localized surface plasmon modes.[8, 12] Therefore, plasmons have ability to enhance radiative emission rate as well as light absorptions which is a primary need for enhancing the performance of polymer based optoelectronic devices such as organic light emitting diodes and solar cells. Despite this, the interaction behaviour is strongly dependent on the electronic structures of organic molecules and metal nanostructure. Silver metal

nanostructure exhibits richness in surface plasmon in comparison to other noble metal. The surface plasmons of metal nanostructures are localized and confined in nanoscale systems. The nanoscale confinement of surface plasmons introduces higher flexibility in tailoring the localized plasmonic properties and also allows for the conjugation of metal nanostructure with organic semiconductor molecules.[12] Thus, in spite of their strong potential for improving device performance and efficiency, there is limited number of reports available on metal nanostructure, simultaneously presenting the enhancement in spectroscopic as well as charge transport properties.

The purpose of this report is to demonstrate the surface plasmons and excitons conjugation effect on spectral as well as charge transport properties of Langmuir-Schaefer (LS) film of Poly (3, 3'''-dialkylquarterthiophene) [PQT-12] over silver nano structure island films (SNIF) deposited on indium tin oxides (ITO) coated glass substrate. PQT-12, has got tremendous attention of researchers as a solution processible polymer for organic electronic devices.[13-16] The long dodecyl chain substituted on the polymer backbone allows extended π-conjugation, making it a suitable semiconductor material. It also holds solution processability, molecular self-organization and liquid crystalline property. The highly regular chain structure causes these regioregular PQT-12 film form lamellar structures with interchain stacking through self-organization into two-dimensional sheets, which is confirmed by X-ray diffraction (XRD) and Scanning tunnelling microscopy (STM) studies.[16-19] These properties of PQT-12 represent an excellent organic device characteristics and make them a model material for easy fabrication of large area electronic devices.[20] Langmuir-Blodgett LB/ Langmuir-Schaefer (LS) technique offers a very excellent way to obtain large area ordered polymer films.[19, 21-23] In this method, the ultra thin film preparation over water surface provides extraordinary control over the thickness of film by layer by layer depositions.[22-23] It also offers a unique approach to prepare smooth ordered thin films of large

area with particular direction oriented and well defined architecture of organic molecule, thus providing a promising and versatile method for constructing large area electronic devices.[24-26] In this study we have used thermal vapour deposition technique[27] as an alternative to traditional chemical route to obtain SNIF. This technique has recently received significant attention to obtain a thin film of metal nanostructures with controlled size and properties, because of its tunable physical, optical and electrical properties.[28] In the present study, we have found that SNIF induce the surface plasmon resonance (SPR) effect both in the spectroscopic as well as charge transport properties of PQT-12 LS film in controlled way and discussed in detail in the following sections.

2. Experimental

2.1 Material Synthesis

The procedure for the synthesis of 3, 3'''–dialkylquarterthiophene monomer and its corresponding polymer molecule have been reported in our previous report (Courtesy to Prof. W. Takashima, KIT, Japan). Dichloromethane (CH_2Cl_2) [Merck, India] was used to isolate the higher molecular weight polymer chains and Soxhlet extraction method were used to extract these molecules as discussed earlier.[29] High purity silver (Ag) wires (99.95% pure) were purchased from Sigma Aldrich chemicals.

2.2 Sample Film Preparation

2.2 (a) Silver Nano-Islands Film (SNIF) Formation:

The nanostructures of Ag over ITO coated glass substrates were obtained by vacuum thermal evaporation/depositions technique at 10^{-6} mbar with the help of model: HIND HIVAC 12A4D. It is important to note that the deposition of ultra thin film (<7 nm) of Ag metal over

solid substrate, temperature of which is less than $1/10^{th}$ of melting point of Ag during deposition cause formations of quenched condense film, which exist in nano size islandic form with charge confinement in thin films ($T_s < 0.1T_m$, where T_s stands for substrate temperature during depositions and T_m stands for melting point of Ag.).[28, 30] Recently, Mishra et. al.[8, 31] observed in their distance dependence surface plasmon coupled metal enhance fluorescence study of eosin, through steady state/ time domain fluorescence measurements and finite difference time domain (FDTD) calculations, that nearly 20 nm thin layer of silver over silica nanoparticles give maximum fluorescence enhancement effect. Therefore, we have deposited only 20 nm thin Ag film with deposition rate of 1 A^0/s and ensured that all time substrate temperature below $1/10^{th}$ of melting point of Ag leads to formation of silver nanostructure islands [SNIF]. For this, we have deposited 5 nm Ag film over ITO substrate by mass transfer and found ~ 20 nm thick SNIF of nearly 40 nm particle size with less than around 25 % surface coverage area, monitored through digital thickness monitor unit (DTM) having quartz crystal microbalance.

2.2. (b) PQT-12 LS Film Formation:

A 0.1mg/ml solution of PQT-12 was made in chloroform and spread over triply deionised water via a 250 μL Hamilton micro syringe (Reno, NV) in the Langmuir trough for study of intermolecular interaction and stability. The film was formed over water surface through compressing the barrier. Before transferring the film over substrate, we have run the three cycles of hysteresis loop of isotherm to obtain a stable configuration over water surface and after that this film transferred over solid substrate by horizontal lifting at constant surface pressure 20 mN/m by using Langmuir Schaefer film deposition system as shown in inset Fig. 1. Bare ITO and SNIF coated over ITO glass slide were used as solid substrate to deposit the LS film of PQT-12. The thickness of different layers of PQT-12 LS films was measured by AFM in line scan mode.

2.3 Device Fabrication:

The charge transport properties of PQT-12 LS film were studied in two kind of sandwiched structures (i) Al/PQT-12 LS/ITO and (ii) Al/PQT-12 LS/SNIF/ITO, respectively. Before the formation of these two devices for charge transport measurement, the ITO substrate was cleaned using deionised water, acetone, and chloroform for 20 minutes each using ultrasonic bath and then baked for 20 minutes in vacuum oven at 50^0C. Aluminium (Al) electrode of size 2 mm x 2 mm at top of polymer films was fabricated by thermal vacuum evaporation unit. The charge transport property measurements of these two sandwiched structures were carried out with source meter of Keithley (model 2612A) at room temperature (27 ^{0}C) in air under dark condition and X-ray photoelectron spectroscopy (XPS) was used for the study of effect of charge transport from PQT 12 LS film to SNIF by change in binding energy through the model Kratos Analytical, SHIMADZU group company AMICUS XPS UK.

2.4 Characterization Tools:

Molecular interaction and stability, studied through pressure (π) vs. area (A) isotherms of PQT-12 LS ultra thin film over water surface by Langmuir trough (Apex Instrument Co. India, model apex 2007 DC). Surface morphology, topography and grain analysis of these films deposited glass substrates were done by using FE-SEM (Quanta-200) and AFM (NT-MTD, Russia), respectively. Samples in AFM were imaged at a scan rate of 1 Hz with 512 × 512 pixel resolution in semi contact mode. Raman spectroscopic measurements were conducted using a Micro Raman Spectrometer at 180^0 scattering geometry (Renishaw, Germany) with 514.5 nm line of Ar^+ laser of 50 mW to investigate the effect of Ag film on PQT 12 LS layer. Absorption spectra of PQT-12 LS film in these substrates were collected using a dual beam spectrophotometer using Perkin Elmer Lamda 25, Germany. Edinberg spectro-fluorometer F-900 was used for steady state and time domain measurement. Front

face sample geometry was used to undertake all the fluorescence emission/ excitation spectra with a slit width of 5 nm, both in the excitation monochromator and emission monochromator with xenon source for excitation. Time-correlated single photon counting (TCSPC) technique, with a red sensitive PMT RS900 was used to measure fluorescence decay curve. The excitation source was a pulsed laser source of wavelength 375 nm having maximum repetition rate 1.0 MHz and pulse duration 1.1 nanosecond (FWHM). The intensity decays were analyzed by decay analysis software (DAS) version 6.4 in terms of the multi-exponential model:

$$I(t) = \sum_i \alpha_i \exp(-t/\tau_i) \qquad (1)$$

where, α_i are the amplitudes and τ_i are the decay times, $\sum_i \alpha_I = 1.0$. The values of α_i and τ_i were determined by nonlinear least square impulse re-convolution analysis with the goodness of fit judged by the residual, autocorrelation function and chi square (χ^2) values. The measurement error in decay time analysis was of the order of ± 0.01 ns. Photo-stability experiments were undertaken using a 530 nm excitation of the sample films through Shimadzu spectrofluoremeter in time scan mode for about 900 sec.

3. Results and discussions

3.1. Pressure (π) Vs. Area (A) Isotherm Study:

Pressure (π) vs. area (A) isotherms of PQT-12 film (0.1 mg/ml in chloroform) spread over water surface were carried out to understand the nature of interaction of molecules, thickness of the monolayer and stability of the film, as shown in Fig. 1. Stability of the LS film over water surface, confirmed by running π-A isotherm several times and a decrease in hysteresis loop area as well as mean monomeric area is observed with repeating the cycles of π-A,

curves two or three times. The first cycle in Fig. 1(a) reveals the large hysteresis loop, however, second and third run retrace almost the same path in their cycle and a successive decrease in loop area indicates the growth and rearrangement of self assembled coplanar molecule of polymer over water surface. The mean monomeric area represented by pressure vs. area isotherm is much less than that of actual monomer for first cycle (Fig. 1(a). This lamella in solutions causes the reduction in area covered by polymer over water surface after spreading. The compressions of the barrier taken place at the time of film formation over water surface because the reductions in area of molecule for compact solid film formation (inset Fig. 1). The effective area of molecules, where it feels interaction is very less in comparison to actual area. This phenomenon indicates the formation of multi molecule thickness film over water surface. Ong et al.[13, 16] has also reported the presence of π-π stacked coplanar molecule lamella in solution for similar kind of molecular chain and the separation between two alkyl chains is 1.2 nm with an angle of 50^0 from backbone and end to end alkyl chains length is 3.28 nm. The calculated area of the monomer is about 3.9 nm^2. On the basis of this calculation, the number of π-π stacked monomer in single layer LS film is found to be around 15 at the onset of isotherm which have also been confirmed by AFM in later section.

3.2 Geometrical and Structural Study:

In order to understand, the structure of PQT-12 monomer and oligomers, geometry optimization of PQT-12 in ground state was carried out by density functional theory (DFT) and Molecular Mechanics (MM) approach using Gaussian 09 [32] program package and Avogadro software[33,] respectively as shown in Fig. 2. For DFT calculation of monomer unit, split valence augmented basis set; singly polarised with (d) polarization function with Becke's exchange functional coupled with gradient-corrected correlation functional of Lee, Yang and Parr[34] [B3LYP/6-31G(d)] was employed. Energy difference between the highest occupied molecular orbital (HOMO) and the lowest unoccupied molecular orbital (LUMO)

was estimated to be 3.52 eV along with dipole moment having value ~ 0.42 Debye. DFT study reveals that PQT-12 monomer is not a planar system, whereas MM calculation, using universal force field (UFF) of oligomer containing four units of monomer, suggests that it attains planar shape in bunch of PQT units.

3.3. Surface Morphology Study:

To understand the surface morphology of the PQT-12 LS sample films, images were scanned under Atomic Force Microscopy (AFM) and Scanning Electron Microscopy (SEM) respectively. Fig. 3 (a), (b), (c) represents 2μm x 2μm area scanned AFM images of silver deposited over ITO coated glass, single layer PQT-12 LS film over ITO coated glass substrate and single layer PQT-12 LS film over silver deposited ITO coated glass slide, respectively. AFM morphology and grain analysis reveals the formation of SNIF of nearly 40 -50 nm size nano-particles (Fig. 3a and Fig. S1). While the AFM topography of PQT-12 single layer LS film over ITO coated glass substrate discloses the formation of very smooth film (Fig. 3b) and its thickness was estimated about 4.8 nm using AFM in line scan mode. The PQT-12 LS film over SNIF deposited on ITO coated glass shows the change in morphology in comparison to PQT-12 LS film without SNIF (Fig. 2c). Further, the results were also confirmed by the SEM, TEM and SAED images as given in supplementary Fig. S2.

3.4 Steady State and Time Domain Fluorescence Study:

Absorption spectrum of SNIF over ITO coated glass is shown in Fig. 4(a). It shows absorption band maxima at 460 nm. The appearance of this absorption band, reveals the formation of nano structure over the solid substrate during the deposition and corresponds to plamonic absorption band of silver. Fig. 4 (b) represents the absorption spectra of PQT-12 LS film over ITO coated glass substrate with and without SNIF, respectively. The appearance of

structured absorption spectra maximum at 531 nm of PQT-12 LS film reveals the rigid molecular structure, and the presence of higher wavelength shoulder peak in PQT-12 LS film indicates the formations of well ordered crystallite domains. The absorption spectra of PQT-12 LS film over SNIF deposited ITO coated glass substrate reveals nearly two fold enhancement in absorbance in comparison to pure PQT-12 LS film over ITO coated glass substrate. It is also observed that the absorbance (optical density) of PQT-12 LS film over both bare ITO coated glass substrate and SNIF deposited ITO coated glass substrate increases linearly with increase in number of layers as shown in figure 4(c). The rate of increase in optical density of Ag coated LS films is more in comparison to PQT-12 LS film over bare ITO substrate. These effects can be explained as a result of the coupling of the PQT-12 dipoles with the localized electromagnetic field of the metallic particles, which efficiently increases the absorption cross-section of the PQT-12. It is well-known that conducting metallic particles can modify the free-space absorption condition in such a way that it increases the incident electric field, felt by fluorophores, effectively increasing the excitation rate of the fluorophore. The enhanced absorption of dye molecules near metallic surfaces was first reported by Glass et al., [35] and also confirmed by other groups.[4-6, 8-9] The absorption spectra of PQT-12 do not show any change in the structure of absorption structural bands on increase in LS layers, which rules out the possibility of dimer or higher aggregate formation in the ground state in this particular polymer. Although, linearity of the absorbance of PQT-12 LS film was preserved up to 14 LS layers as shown in Fig. 4 (c), but in fluorescence measurement, it is observed that 12 LS layers of PQT-12 (thickness ~ 58 nm) on SNIF, shows maximum fluorescence enhancement. Therefore, we use this sample film as an optimized one for all farther spectral and charge transport measurements.

The fluorescence excitation and emission spectra of 12 LS layers of PQT-12 film over ITO coated glass with and without SNIF are shown in Fig. 5. It shows a red fluorescence

band maximum at 665 nm in bare ITO LS film, whereas, nearly six fold enhancement is observed in this band of PQT-12 LS film on SNIF deposited ITO coated glass substrate, excited by 530 nm [Fig. 5 (b)]. The enhancement factor is defined as the ratio of intensity observed from SNIF (near-field) divided by that from without SNIF, control PQT12 LS film over ITO coated glass substrate under otherwise identical conditions. To confirm the origin of the fluorescence, excitation spectra were measured by monitoring the emission at blue and the red edges of the fluorescence band, where no change was observed in the excitation spectra, subsequently ruling out the potential formation of any ground state complex. Further, in SNIF containing PQT-12 polymer films, the intensity of the excitation band increases nearly two times with respect to the bare LS film on ITO coated glass substrate; this enhancement in excitation spectra [Fig. 5 (a)] resembles the absorption spectra, as shown in Fig. 4 (b).

Further, in order to understand the above spectral enhancement of PQT-12 LS film near SNIF surface over ITO coated glass substrate, time resolved fluorescence measurements were also carried out using TCSPC technique. The analyzed decay data are given in table 1 and the corresponding analyzed overlapped time resolved decay curves are shown in Fig. 6. The goodness of fitting of the collected decay was judged by the distribution of residuals and associated chi-square values.

Table 1. Time Resolved Fluorescence Decay Parameters of PQT-12 LS Film.

Sample λ_{Ex} **530 nm /** λ_{Em} **665nm**	τ_1 **(ns)**	α_1 **%**	τ_2 **(ns)**	α_2 **%**	τ_3 **(ns)**	α_3 **%**	$\langle\tau\rangle^a$ **(ns)**	$\bar{\tau}^b$ **(ns)**	$\chi 2$
PQT-12 LS/ITO/glass	0.05	81	0.52	20	2.07	7	0.29	0.35	1.251
PQT-12 LS/SNIF/ITO/glass	0.03	69	0.45	24	2.03	5	0.23	0.26	1.276
PQT-12 LS/SNIF/ITO/glass + External electric field	0.01	65	0.40	33	1.37	2	0.17	0.09	1.210

[a] $\langle\tau\rangle$ is the amplitude weighted decay time $\Sigma\tau_i\alpha_i$, and [b] $\bar{\tau}$ is the mean decay time $\Sigma\tau^2{}_i\alpha_i,/ \Sigma\tau_i\alpha_i$,

It is observed that PQT-12 LS film decays triple-exponentially, with an average decay time of 0.35 ns and amplitude weighted decay time 0.29 ns in LS film, these values decreases to 0.26 ns and 0.23 ns respectively in the presence of SNIF. These reductions in decay times of PQT-12 in the presence of SNIF indicate the coupling of excited states of PQT-12 molecules with surface plasmons of the SNIF and the subsequent nonradiative energy transfer among them, consistent with the radiative plasmonic model postulated by Geddes and Lakowicz.[1]

These observations are modifications to the classical far-field (≥1 wavelength of light away) rate equations. The free-space quantum yield (Q_0) and decay time (τ_0) for a fluorophore is given by:[4]

$$Q_0 = \frac{\Gamma}{\Gamma + k_{nr}} \qquad (2a)$$

and

$$\tau_0 = \frac{1}{\Gamma + k_{nr}} \qquad (2b)$$

where, Γ is the radiative rate and k_{nr} is the non-radiative rate. In this free-space condition, any changes in a fluorophore radiative rate invariably result in the quantum yield and lifetime, Q_0 and τ_0, respectively, changing in unison. However for SPC-MEF, these classical far-field conditions get modified for the near-field condition, such that:

$$Q_m = \frac{\Gamma + \Gamma_m}{\Gamma + \Gamma_m + k_{nr}} \qquad (3a)$$

and $$\tau_m = \frac{1}{\Gamma + \Gamma_m + k_{nr}} \qquad (3b)$$

where, Q_m and τ_m are the metal modified quantum yield and lifetime, respectively. On analysing the above results, we subsequently propose that there are two populations of adsorbed PQT-12 LS film on the SNIF containing LS film: one set of population is composed of more isolated molecules far from the SNIF, and the photophysical properties of these are similar to PQT-12 in the far-field or free space condition. However, in another set of

population, near SNIF, i.e. in the near field an enhanced absorption and coupling to plasmons, facilitates metal enhanced PQT-12 fluorescence as well as an enhanced photo-stability with reduced decay time.

Further, in order to understand metal-enhanced PQT-12 LS fluorescence dynamics, we have also measured the photostability of PQT-12 in LS films with and without SNIF deposited ITO coated glasses substrate. These samples were exposed by 531 nm radiation from xenon lamp, for about 900 seconds and the steady state fluorescence was measured as a function of time (Fig. 7). The photostability of the PQT-12 is found more pronounced on SNIF containing LS film as compared to the LS film control, i.e. more photons are observed per unit time (photon flux). This finding of enhanced fluorescence photostability is consistent with the reduced decay time of PQT-12 near-to SNIF (Table 1).

Interestingly, it is also observed that on applying the external electrical field on the PQT-12 LS film on SNIF deposited ITO coated glass substrate, both the fluorescence intensity [Fig. 5 b (iii)] and decay time [Fig. 6 (c)] of 665 nm emission band decreases by 530 nm excitation [Table 1]. This result indicates the surface plasmon coupled metal enhanced fluorescence intensity which can further be enhanced and controlled by external electric field and can be used more efficiently for the development of organic LED. Similar decrease in fluorescence intensity of fluorophor with applied external electric field reported by Geddes and Co workers [36-37] in their voltage gated metal enhanced fluorescence studies in semi continues silver nanoparticle film.

3.5 Surface Plasmon Enhance Raman Study:

Raman spectra of SNIF deposited on ITO coated glass substrate along with PQT-12 LS film deposited over, with and without SNIF deposited ITO coated glass substrate are shown in Fig. 8. SNIF deposited film does not show any Raman peak [Fig. 8 (a)] while extremely

weak Raman signal is observed in PQT-12 LS film deposited over ITO coated glass substrate [Fig. 8 (b)]. The observed peaks at 1457 cm^{-1}, 1393 cm^{-1} and 1057 cm^{-1} corresponds to C=C symmetrical stretching, ring C-C stretching and C-H bending vibrations, respectively. Interestingly, huge enhancement in intensity of these Raman signals of PQT-12 LS film is observed in SNIF deposited ITO glass slide along with appearance of an additional peak at 1565 cm^{-1} which correspond to C=C asymmetric stretching mode of vibration. Nearly, thirteen fold enhancement is observed in C=C symmetrical stretching mode (1457 cm^{-1}) of Raman signal. The magnitude of enhancement in Raman signal of PQT-12 vibrations in this case is very less (~13 fold) in comparison to electromagnetic near field effect for isolated system (should be nearly 1000 fold).[38] This again indicates the formation of plasmon coupled fluorophor unified system due to adsorption of PQT-12 LS film over SNIF. It is probably, because of chemical enhancement of surface plasmon enhance Raman signal by inter molecular interaction.

3.6 Charge Transport Property

Charge transport properties of PQT-12 LS film, over without (Al /PQT-12/ITO) and with SNIF deposited ITO coated glass substrate (Al/PQT-12/ SNIF/ITO) devices were studied by measuring the current density (J) vs. voltage (V) characteristics in Schottky diode configurations as shown Fig. 9. The thickness of PQT-12 LS layer remains same in all configurations. The J-V characteristic in all configurations shows the non linear behaviour and follows the thermionic emission Schottky equations as follows [39-40]

$$J = J_0\left[\exp\left(\frac{qV}{\eta kT}\right) - 1\right] \qquad (4)$$

where, η is ideality factor, k is Boltzmann constant, T is temperature, q is charge, V is voltage and J_0 is saturation current density given as:

$$J_0 = AT^2\left[\exp\left(-\frac{q\Phi_B}{kT}\right)\right] \quad (5)$$

where, Φ_B is barrier height between Al and polymer.

$$\eta = \frac{q}{kT}\left[\frac{\partial V}{\partial \ln J}\right] \quad (6)$$

On the basis of above equations different charge transport parameters viz. ideality factor, saturation current density and barrier height calculated from J-V characteristics in different device films are shown in table 2.

Table 2: Electronic parameters of device performance under different condition.

Devices	**Ideality Factor**	**J_0(A/cm^2)**	**Φ_B (eV)**
ITO/PQT-12 /Al	4	2.5x10^{-9}	1.09
ITO/SNIF/PQT-12 LS /Al	2.5	1.7x10^{-5}	0.84
ITO/SNIF/PQT-12 LS/ Al +Laser light	2.3	2.0 x10^{-4}	0.83

PQT-12 LS film shows nearly 1.5 μA/ cm^2 current density over ITO coated glass substrate (Al /PQT-12/ITO) [Fig. 9(a)], while enhancement in current density of the order of 10^3 with better ideality factor in ITO/SNIF/PQT-12 LS/Al configuration is observed, with increase in both reverse saturation current density and decrease in barrier height (Fig. 9(b)). The illuminations of Al/PQT-12LS/ SNIF/ITO junctions from ITO side with green laser light shows the further enhancement in current density in comparison to the un-illuminated junction with further improved ideality factor as shown in Fig. 9 (c).

Further, in order to understand enhancement in spectral as well as in current density of PQT-12 LS film, X-ray photoelectron spectral measurement of SNIF were carried out with and without PQT-12 LS film over the surface of SNIF. XPS spectra of thermally coated

SNIF, without and with LS film of PQT-12 are shown in Fig. 9. In bare SNIF, $3d_{3/2}$ and $3d_{5/2}$ binding energy transitions of Ag are observed at 378 eV and 372.5 eV, respectively. However, on layering the PQT-12 LS film over SNIF, both the binding energy transition of silver are red shifted with decrease in intensity. This again confirms the formation of fluorophore-plasmon coupled unified system of PQT-12 LS with silver nanostructures, by chemi-adsorption (through week Wander-Wall forces), therefore partial charge transfer from PQT-12 polymer backbone to SNIF take place and cause reduction in binding energy which induces enhancement in conductivity. This again supports the coupling of surface plasmons of SNIF with conducting fluorescent polymer PQT-12 LS film.

Finally, on summarizing above results, the current interpretation of surface plasmon coupled metal enhance fluorescence of PQT-12 LS film near the SNIF, supports the radiating plasmon model (RPM), proposed by Geddes and Lakowicz,[4-5] whereby non-radiative energy transfer occurs from excited fluorophores to surface plasmons in non-continuous films due to fluorophore-plasmon near field coupling. The surface plasmons in turn, efficiently radiate the emission of the coupling fluorophores through the scattering portion of the SNIF extinction spectrum and controlled by external electric field as shown in scheme I. Appearance of an increase in the fluorescence emission from the plasmon-fluorophore unified system with the spectral properties of the fluorophores maintained, and a reduction in the fluorescence decay time, giving rise to improvements in the photo stability of the PQT-12 LS film. These results show that near-field surface plasmons are capable to enhance and control; both spectral as well as charge transport properties of PQT-12-LS film and provide, a new approach in the next generation of energy efficient materials for multifarious applications.

4. Conclusions

The present work describes near-field effects of SNIF both on spectral and charge transport properties of LS film of PQT-12 on ITO coated glass substrate. In the near field, i.e. near SNIF, coupling of plasmons with PQT-12 LS film enhances both absorption and fluorescence as well as facilitates to enhanced photo-stability with decrease in decay time as compared to an identical control sample containing no silver i.e. the far field condition. The photo-physical and charge transport properties of PQT-12 are found to be both drastically and favourably changed near the metallic nanoparticle surfaces in such a way that an opportunity to develop a highly novel platform approach for the voltage controlled electro-luminescent materials with a higher photon flux can be realized.

Supporting information available: Particle size analysis using AFM histogram given in Fig.S1 and SEM image of PQT-12 LS film (a) Single Layer over ITO, (b) Double layer over ITO, (c) Double layer LS film deposited over SNIF, (d) SNIF, (e) TEM image of single layer LS film and (f) SAED pattern are given in supplementary Fig. S2.

Acknowledgements

Authors acknowledge the Department of Physics, BHU Varanasi for Time domain fluorescence measurement and are also thankful to U.G.C. and MHRD New Delhi for financial support.

References

1. H. Choi, S.J. Ko, Y. Choi, P. Joo, T. Kim, B. R. Lee, J.W. Jung, H. J. Choi, M. Cha, J.-R. Jeong, I.W. Hwang, M. H. Song, B. S. Kim and J. Y. Kim*, Nat. Photon,*. 2013*,* **7**, 732.

2. M. Heo, H. Cho, J.W. Jung, J.R. Jeong, S. Park, and J. Y. Kim, *Adv. Mater.,* 2011, **23**, 5689.
3. H. A. Atwater, and A. Polman, *Nat. Mater*. 2010, **9**, 205.
4. C. D. Geddes and J. R. Lakowicz, *J. Fluorescence*, 2012, **12**, 121.
5. "Radiative decay engineering"- Topic in fuoroscence spectroscopy Vol. 8 edited by C. D. Geddes, and J. R. Lakowicz, Spriger, Newyork 2004.
6. Metal Enhanced Fluorescence. Ed. C. D. Geddes; 2010 Wiley International, USA.
7. H. Mishra, and C. D. Geddes, *J. Phys. Chem. C*, 2014, **118**, 28791.
8. H. Mishra, A. Dragan, and C. D. Geddes, *J. Phys. Chem. C,* 2011, **115**, 17227.
9. H. Mishra, Y. Zhang and C. D. Geddes, *Dyes and Pigments,* 2011, **91**, 225.
10. Y.-C. Ho, S.-H. Kao, H.-C. Lee, S.-K. Chang, C.-C. Lee and C.-F. Lin, *Nanoscale*, 2015, **7**, 776.
11. A. Kumar, R. Srivastava, P. Tyagi, D.S. Mehta, and M.N. Kamalasanan, *Organ. Electron.*, 2012, **13**, 159.
12. H. Chen, T. Ming, L. Zhao, F. Wang, L.-D. Sun, J. Wang and C. H. Yan, *Nano Today,* 2010, **5**, 494.
13. B. S. Ong, Y. Wu, P. Liu, and S. Grardner, *Adv. Mater*. 2005, **17**, 1141.
14. R. K. Pandey, A. K. Singh, and R. Prakash, *J. Phys. Chem. C* 2014, **118**, 22943.
15. S. Kuehn, P. Pingel, M. Breusing, T. Fisher, J. Stumpe, D. Neher, and T. Elsesser, *Adv. Funct. Mater.*, 2011, **21**, 860.
16. B. S. Ong, Y. Wu, P. Liu, and S. Gardner, *J. Am. Chem. Soc.,* 2004, **126**, 3378.
17. P. Keg, A. Lohani, D. Fichou, Y. M. Lam, Y. Wu, B. S. Ong and S. G. Mhaisalkar, *Macromol. Rapid Commun*., 2008, **29**, 1197.
18. N. Zhao, G. A. Botton, S. Zhu, A. Duft, B. S. Ong, Y. Wu, and P. Liu, *Macromolecules* 2004, **37***,* 8307.

19. R. K. Pandey, A. K. Singh, C. Upadhyay, and R. Prakash, *J. Appl. Phys.* 2014, **116**, 094311.

20. C. D. Dimitrakopoulos, and P. R. L. Malenfant, *Adv. Mater*. 2002, **14**, 99.

21. R. K. Pandey, C. Upadhyay, and R. Prakash, *RSC Adv.,* 2013, **3**, 15712.

22. D. Natall, M. Sampietro, L. Franco, A. Bolognesi and C. Botta, *Thin Solid Films,* 2005, **472**, 238.

23. G. Xu, Z. Bao, and J. T. Groves, *Langmuir*, 2000, **16***,* 1834.

24. Z. Zhang, K. Nakashima, A. L. Verma, M. Yoneyama, K. Iriyama, and Y. Ozaki, *Langmuir,* 1998, **14***,* 1177.

25. A. L. Verma, Z. Zhang, N. Tamai, K. Nakashima, M. Yoneyama, K. Iriyama, and Y. Ozaki*, Langmuir,* 1998, **14***,* 4638.

26. D. T. McQuade, J. Kim, and T. M. Swager*, J. Am. Chem. Soc*., 2000, **122**, 5885.

27. K. L. Ekinci and J. M. Valles, Jr., *Phys. Rev. B,* 1998, **58**, 7347.

28. K.-C. Lee, S. –J. Lin, C.-H. Lin, C.-S. Tsai and Y.-J. Lu, *Surf. Coat. Tech., 2008***, 202**, 5339.

29. R. K. Pandey, W. Takashima, S. Nagamatsu, A. Deaundorffer, K. Kaneto, and R. Prakash, *J. Appl. Phys*., 2013, **114**, 054309.

30. C. A. Neugebauer and M. B. Webb, *J. App. Phy.,* 1962, **33**, 74.

31. H. Mishra, B. Mali, J. Karoline, A, I. Dragen and C.D. Geddes, *Phy. Chem. Chem. Phys*, 2013,**15**, 19538.

32. M. J. Frisch, G. W. Trucks, H. B. Schlegel, G. E. Scuseria, M. A. Robb, J. R. Cheeseman, G. Scalmani, V. Barone, B. Mennucci, G. A. Petersson, H. Nakatsuji, M. Caricato, X. Li, H. P. Hratchian, A. F. Izmaylov, J. Bloino, G. Zheng, J. L. Sonnenberg, M. Hada, M. Ehara, K. Toyota, R. Fukuda, J. Hasegawa, M. Ishida, T. Nakajima, Y. Honda, O. Kitao, H. Nakai, T. Vreven, J. A. Montgomery Jr, J. E.

Peralta, F. Ogliaro, M. Bearpark, J.J. Heyd, E. Brothers, K. N. Kudin, V. N. Staroverov, T. Keith, R. Kobayashi, J. Normand, K. Raghavachari, A. Rendell, J. C. Burant, S. S. Iyengar, J. Tomasi, M. Cossi, N. Rega, J. M. Millam, M. Klene, J. E. Knox, J. B. Cross, V. Bakken, C. Adamo, J. Jaramillo, R. Gomperts, R. E. Stratmann, O. Yazyev, A. J. Austin, R. Cammi, C. Pomelli, J. W. Ochterski, R. L. Martin, K. Morokuma, V. G. Zakrzewski, G. A. Voth, P. Salvador, J. J. Dannenberg, S. Dapprich, A. D. Daniels, O. Farkas, J. B. Foresman, J. V. Ortiz, J. Cioslowski, and D.J. Fox (2010) Gaussian 09, revision B.01. Gaussian, Inc., Wallingford, CT

33. M. D. Hanwell, D. E Curtis, D. C Lonie, T. Vandermeersch, E. Zurek and G. R Hutchison; "Avogadro: An advanced semantic chemical editor, visualization, and analysis platform" *J. Cheminfo.* 2012, **4,** 17.
34. C. Lee, W. Yang, and R. G. Parr, *Phys. Rev. B*, 1998, **37**, 785.
35. A.M Glass, P.F. Liao, J.G. Bergman, D.H. and Olson,; Opt. Lett. 1980, **5** 368.
36. A. I. Dragan , Y. Zhang and C. D. Geddes, *J Fluoresc*, 2009, **19**, 369.
37. Y. Zhang, K. Aslan and C. D. Geddes, *J. Fluoresc*, 2009, **19**,363.
38. M. M. Maitani, D. A. A. Ohlberg, Z. Li, D. L. Allara, D. R. Stewart, and R. S. Williams, *J. Am. Chem. Soc.* 2009, **131**, 6310.
39. R. K. Pandey, A. K. Singh, R. Prakash, *AIP Adv.,* 2013, **3**, 122120.
40. A. K. Singh, A. D. D. Dwivedi, P. Chakrabarti, R. Prakash, *J. Appl. Phys.* 2009, *105*, 114506.

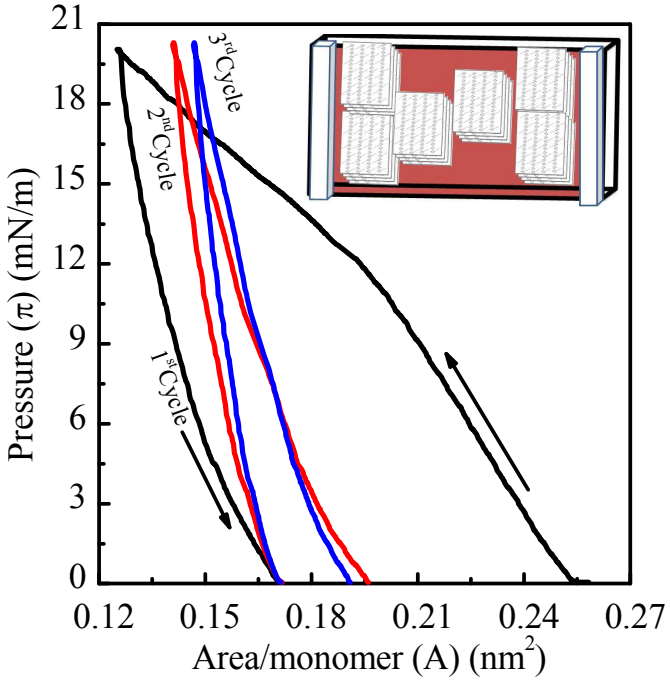

Fig. 1. Pressure (π) vs. area (A) isotherm of PQT-12 in chloroform [concentration 0.1 mg/ml]. (Inset shows the schematic diagram of Langmuir trough with PQT-12 molecule lamella.

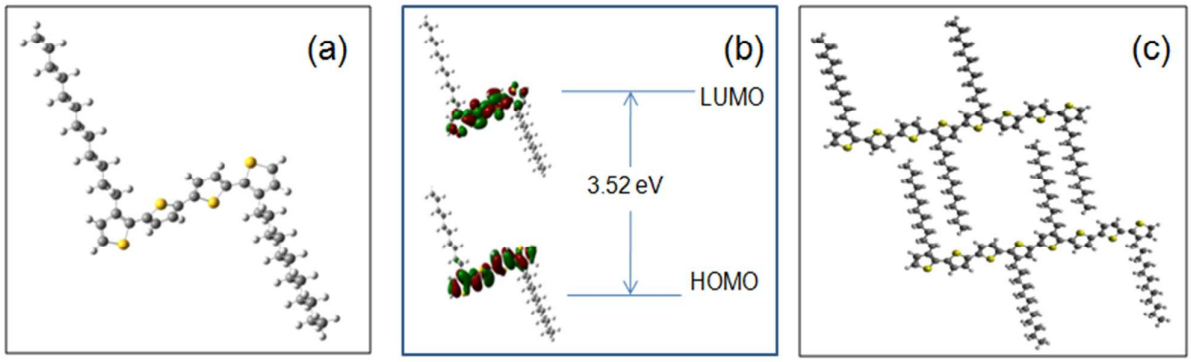

Fig. 2. Optimized geometry of PQT-12 (a) monomer at B3LYP/6-31G* level of DFT theory, (b) HOMO-LUMO band gap and (c) PQT-12 oligomer at MM/UFF level of theory.

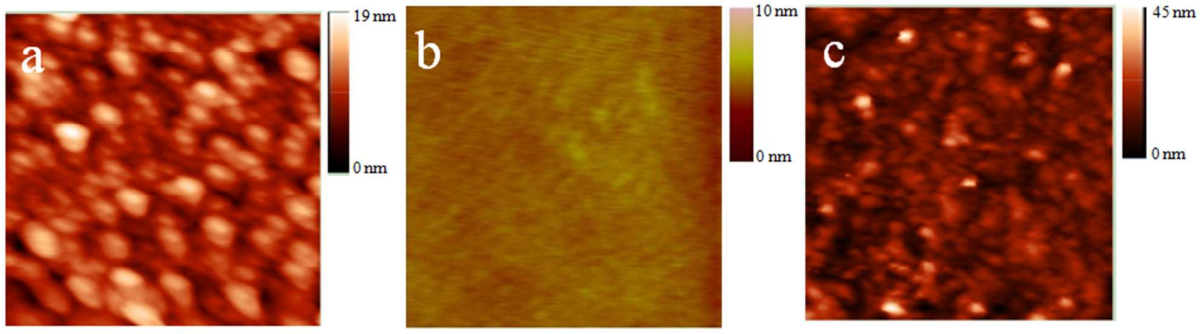

Fig. 3. Atomic force microscopy (2µm x 2µm) image of (a) silver film (SNIF) (b) single layer PQT-12 LS film (c) single layer PQT-12 LS film on SNIF.

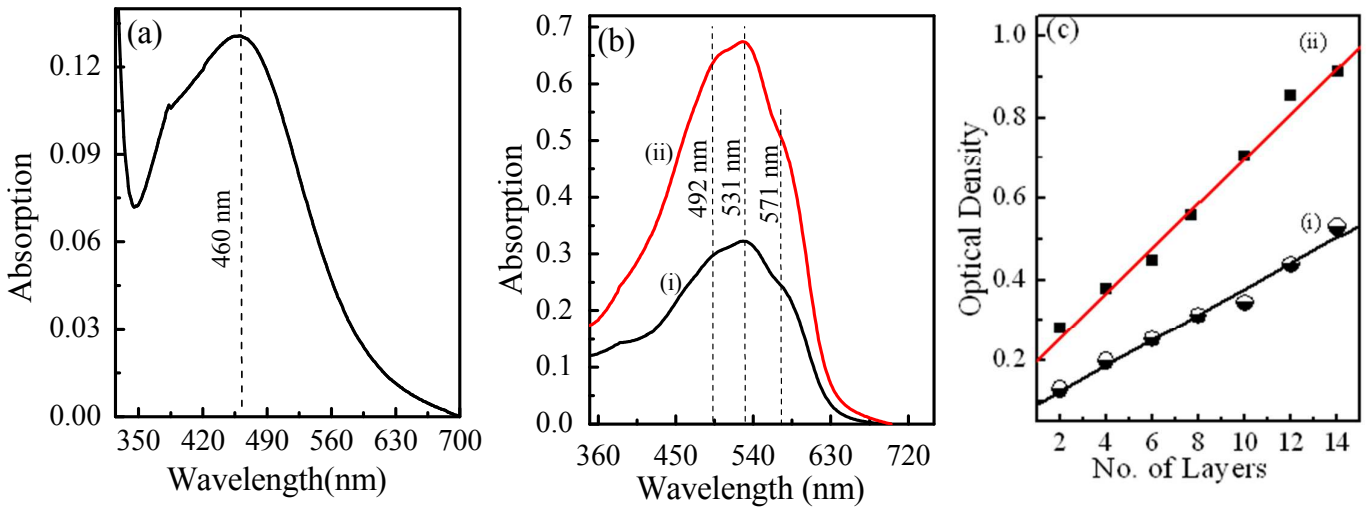

Fig. 4. Absorption spectrum of (a) SNIF layer (b) PQT-12 LS film (i) without SNIF layer (ii) with SNIF layer on ITO coated glass substrate (c) Optical density vs. No. of layer on ITO coated glass substrate (i) without SNIF and (ii) with SNIF layer.

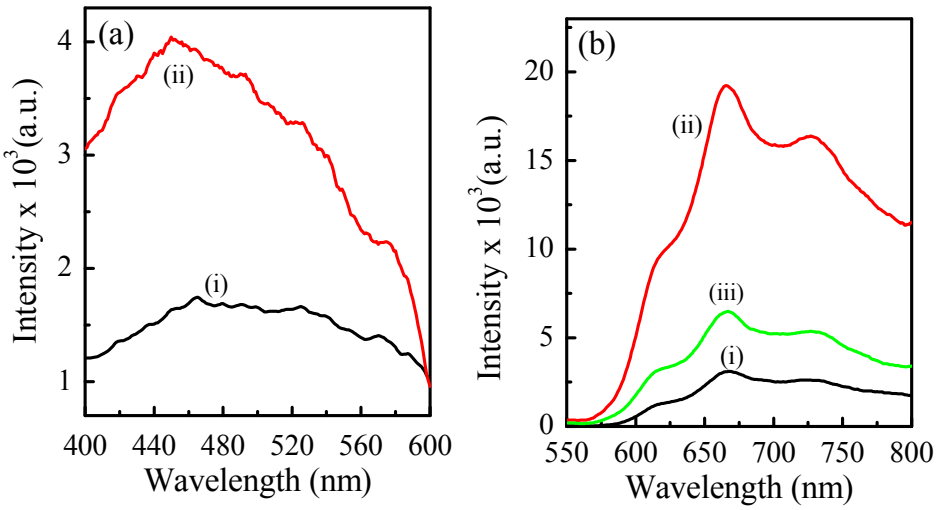

Fig. 5. Fluorescence (a) excitation spectrum [λ_{em} = 665 nm] and (b) emission spectrum [λ_{ex} = 530 nm] of 12 layers LS film of PQT-12 on ITO coated glass (i) without SNIF layer and (ii) with SNIF layer (iii) with SNIF layer + Electric field.

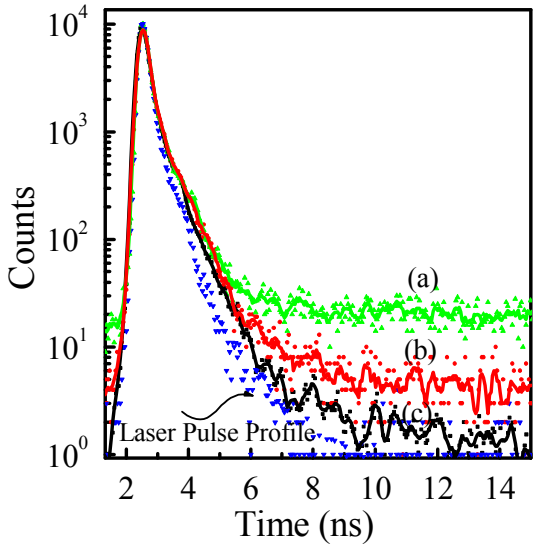

Fig. 6. Fluorescence decay curves of 12 layers LS film of PQT-12 on ITO coated glass (a) without SNIF layer and (b) with SNIF layer (c) with SNIF layer and external electric field. (λ_{em} = 375 nm).

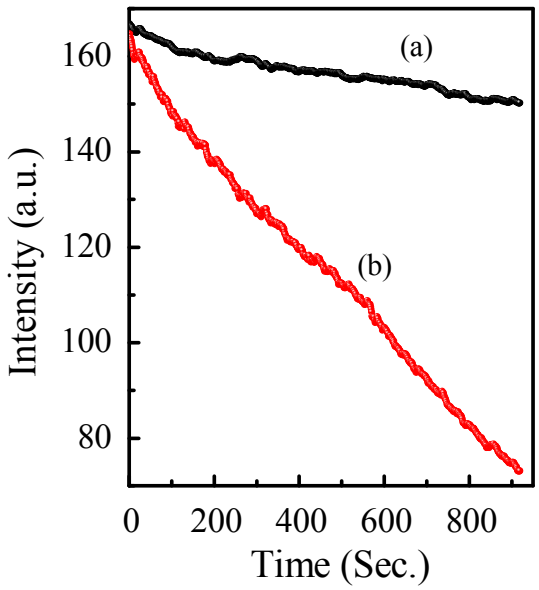

Fig.7. Photo stability curves of 12 layers LS film of PQT-12 on ITO coated glass (a) With SNIF layer (b) without SNIF layer.

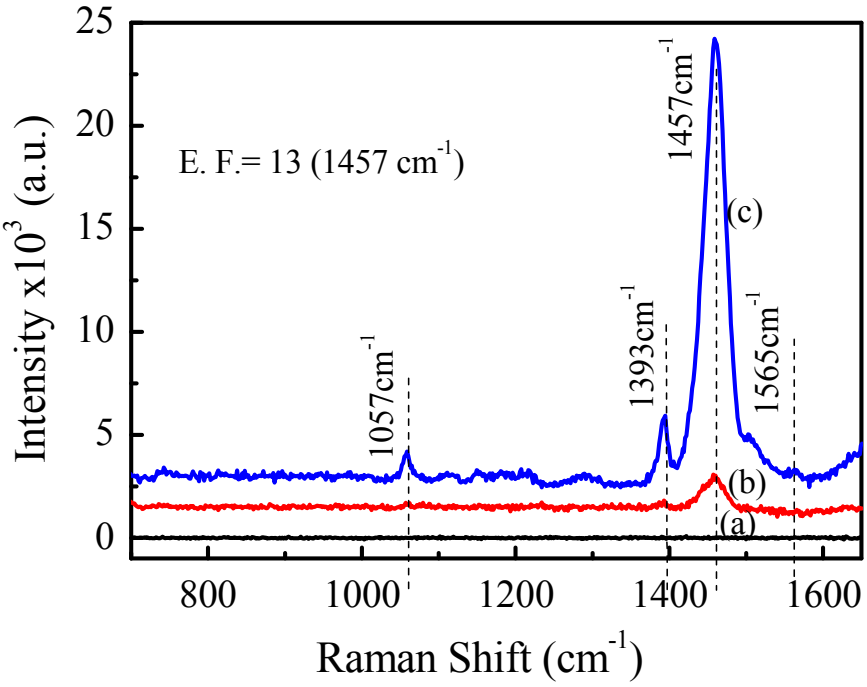

Fig.8. Raman spectra of (a) SNIF (b) 12 layers LS film of PQT-12 without SNIF layer and (c) 12 layers LS film of PQT-12 with SNIF layer.

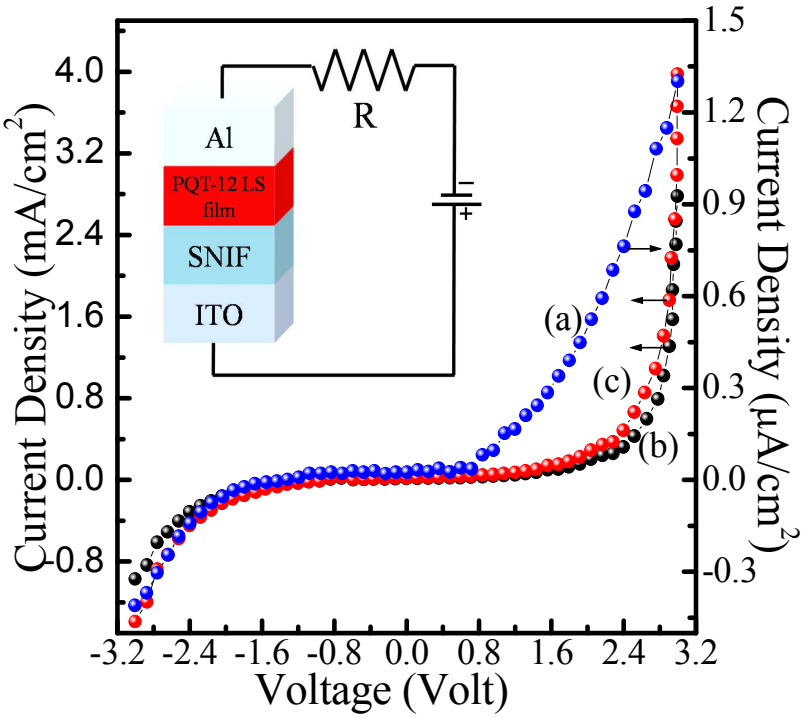

Fig. 9:- Current density (J)- Voltage (V) characteristics of 12 layers LS film of PQT-12 (a) without SNIF (b) with SNIF, and (c) with SNIF irradiated by green laser light (λ = 520 nm).

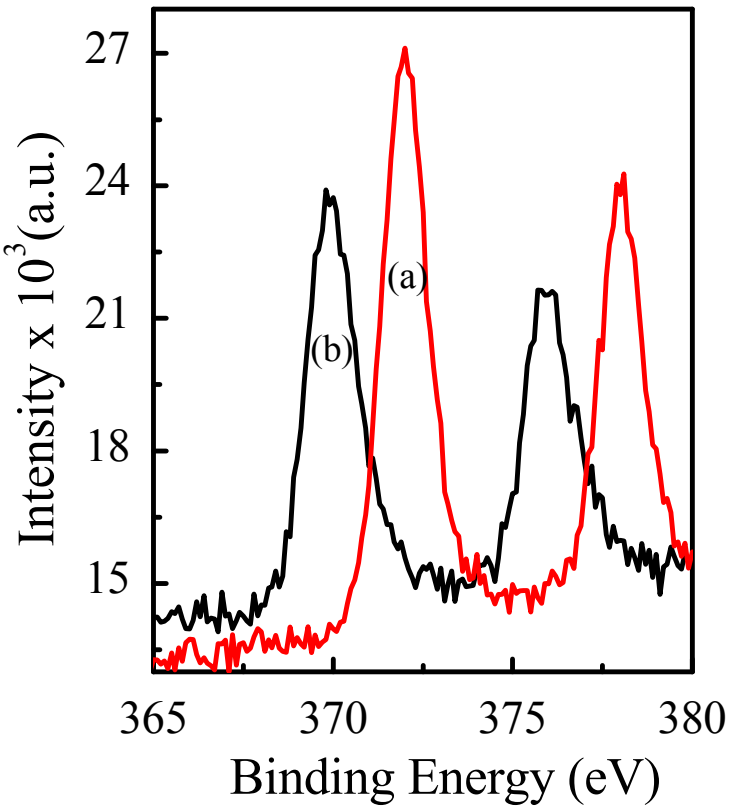

Fig.10. X-ray photoelectron spectroscopy of thermally coated SNIF (a) without and, (b) with PQT-12 LS film.

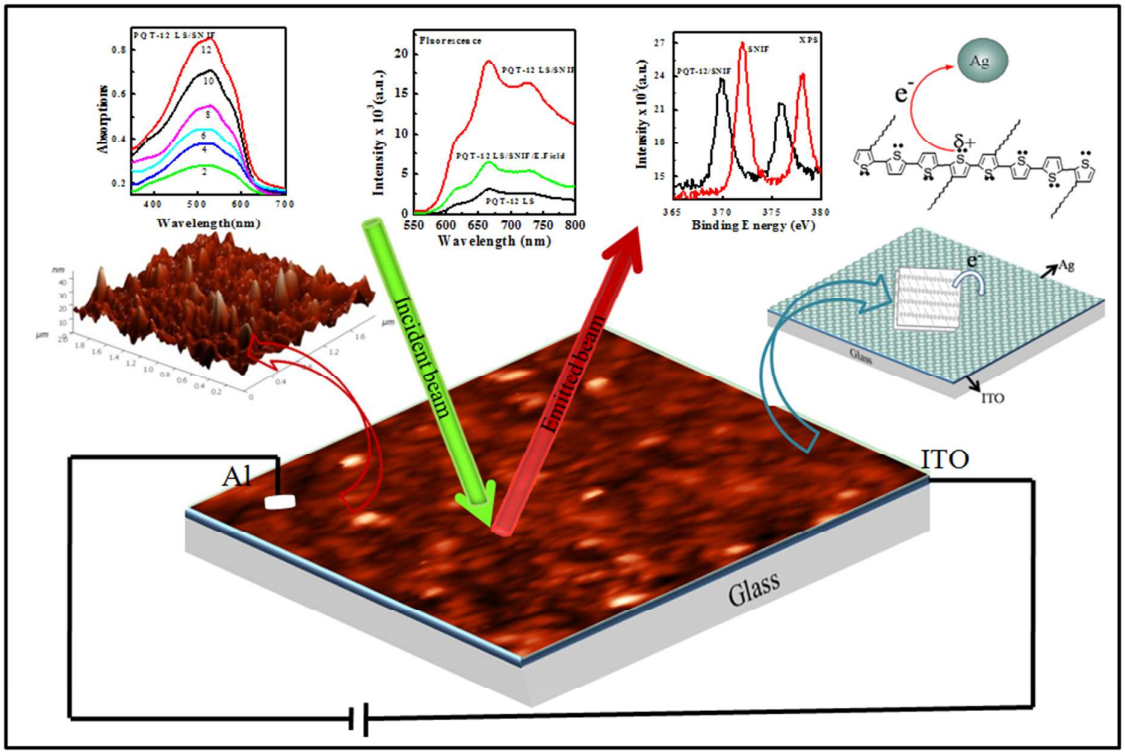

Scheme I: Cartoon depicting the sample device geometry used to study the Surface Plasmon coupled Metal Enhanced Spectral and transport properties of Poly (3, 3‴-dialkylquarterthiophene) Langmuir Schaefer Film.